PHYSICAL REVIEW A **77**, 030101(R) (2008)

Nonmonotonic effects of parallel sidewalls on Casimir forces between cylinders

Sahand Jamal Rahi,[1] Alejandro W. Rodriguez,[1] Thorsten Emig,[2,3] Robert L. Jaffe,[4] Steven G. Johnson,[5] and Mehran Kardar[1]

[1]*Department of Physics, Massachusetts Institute of Technology, Cambridge, Massachusetts 02139, USA*

[2]*Institut für Theoretische Physik, Universität zu Köln, Zülpicher Strasse 77, 50937 Köln, Germany*

[3]*CNRS, LPTMS, UMR8626, Bât. 100, Université Paris-Sud, 91405 Orsay, France*

[4]*Center for Theoretical Physics and Laboratory for Nuclear Science, Massachusetts Institute of Technology, Cambridge, Massachusetts 02139, USA*

[5]*Department of Mathematics, Massachusetts Institute of Technology, Cambridge, Massachusetts 02139, USA*

(Received 13 November 2007; published 13 March 2008)

We analyze the Casimir force between two parallel infinite metal cylinders with nearby metal plates using two methods. Surprisingly, the attractive force between cylinders depends nonmonotonically on the separation from the plate(s), and the cylinder-plate force depends nonmonotonically on the separation of the cylinders. These multibody phenomenona do not follow from simple two-body force descriptions. We can explain the nonmonotonicity with the screening (enhancement) of the interactions by the fluctuating charges (currents) on the two cylinders and their images on the nearby plate(s).

DOI: 10.1103/PhysRevA.77.030101 PACS number(s): 12.20.Ds, 42.50.Ct, 42.50.Lc

Casimir forces arise from quantum vacuum fluctuations, and have been the subject of considerable theoretical and experimental interest [1–4]. We consider here the force between metallic cylinders with one or two parallel metal sidewalls (Fig. 1) using two independent exact computational methods, and find an unusual nonmonotonic dependence of the force on the sidewall separation. These nonmonotonic effects cannot be predicted by commonly used two-body Casimir-force estimates, such as the proximity-force approximation (PFA) [5,6] that is based on the parallel-plate limit, or by addition of Casimir-Polder "atomic" interactions (CPI) [6–8].

In previous work, we demonstrated a similar nonmonotonic force between two metal squares in proximity to two parallel metal sidewalls, for either perfect or realistic metals [9]. This work, with perfect-metal cylinders [10], demonstrates that the effect is not limited to squares (i.e., it does not arise from sharp corners or parallel flat surfaces), nor does it require two sidewalls. The nonmonotonicity stems from a competition between forces from transverse electric (TE) and transverse magnetic (TM) field polarizations: In the latter case, the interaction between fluctuating charges on the cylinders is screened by opposing image charges, in the former case it is enhanced by analogous fluctuating image currents. Furthermore, we show that a related nonmonotonic variation arises for the force between the cylinders and a sidewall as a function of separation between the cylinders, a geometry potentially amenable to experiment.

Casimir forces are not two-body interactions: quantum fluctuations in one object induce fluctuations throughout the system, which in turn act back on the first object. However, both the PFA and CPI view Casimir forces as the result of attractive two-body ("pairwise") interactions. They are reasonable approximations only in certain limits (e.g., low curvature for PFA), and can fail qualitatively as well as quantitatively otherwise. Pairwise estimates fail to account for two important aspects of the Casimir forces in the geometry we consider [11]. First, a monotonic pairwise attractive force clearly cannot give rise to the nonmonotonic effect of the sidewalls. Second, the application of either method here would include two contributions to the force on each cylinder: attraction to the other cylinder and attraction to the sidewall(s). If the latter contribution is restricted to the portion of the sidewall(s) where the other cylinder does not interpose ("line of sight" interactions), the cylinder will experience greater attraction to the opposite side, thereby *reducing* the net attractive force between the cylinders [11]. In contrast, exact calculations predict a nonmonotonic force that is *larger* in the limit of close sidewalls than for no sidewalls. These important failures illustrate the need for caution when applying uncontrolled approximations to new geometries even at the qualitative level. (On the other hand, a ray-optics approximation, which incorporates nonadditive many-body ef-

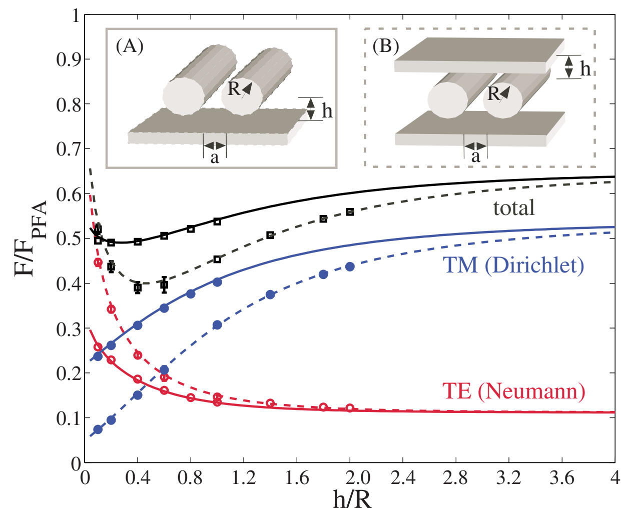

FIG. 1. (Color online) Casimir force per unit length between two cylinders (black) vs the ratio of sidewall separation to cylinder radius h/R, at fixed $a/R=2$, normalized by the total PFA force per unit length between two isolated cylinders [$F_{\mathrm{PFA}}=\frac{5}{2}(\hbar c\pi^3/1920)\sqrt{R/a^7}$ [18]]. The solid lines refer to the case with one sidewall, while dashed lines depict the results for two sidewalls, as indicated by the inset. Also shown are the individual TE (red) and TM (blue) forces.

fects, at least qualitatively predicts these features for the case of two square and/or sidewall [11].)

The insets in Fig. 1 illustrate the three-dimensional geometries that we consider: two infinite, parallel, perfect-metal cylinders of radius R separated by a distance a (center-to-center separation $2R+a$) and oriented along the z axis, with one [Fig. 1(A)] or two [Fig. 1(B)] infinite metal sidewall(s) parallel to the cylinders and separated from both by equal distance h ($h+R$ to the cylinder axes). For perfectly conducting objects with z-translational symmetry, the electric (**E**) and magnetic (**H**) fields can be decomposed into TE and TM polarizations, described by scalar fields ψ satisfying Neumann (TE, $\psi=H_z$) and Dirichlet (TM, $\psi=E_z$) boundary conditions at the metallic surfaces [12].

To analyze these geometries, we employ two complementary and exact computational methods, based on path integrals (PI) and the mean stress tensor (ST). The methods are *exact* as they involve no uncontrolled approximations and can yield arbitrary accuracy given sufficient computational resources. They are *complementary* in that they have different strengths and weaknesses. The PI method is most informative at large separations where it leads to analytical asymptotic expressions. The ST method, while relatively inefficient for large separations or for the specific geometries where PI is exponentially accurate, is formulated in a generic fashion that allows it to handle arbitrary complex shapes and materials without modification. As both methods are described in detail elsewhere [13,14], we only summarize them briefly here. The present geometry provides an arena where both methods can be applied and compared.

In the PI approach, the Casimir force is calculated via the constrained partition function. The Dirichlet (Neumann) constraints on the TM (TE) fields are imposed by auxiliary fields on the metallic surfaces [15] which can be interpreted as fluctuating charges (currents). The interaction between these charges is related to the free-space Green's functions—the addition of metallic sidewall(s) merely requires using image charges (currents) to enforce the appropriate boundary conditions. The calculations are further simplified by using Euclidean path integrals and the corresponding imaginary-frequency $\omega=iw$ Green's function. In the case of infinite cylinders, these surface fields can be represented in terms of a spectral basis: their Fourier series, leading to Bessel functions in the Green's function [5,10,16]. An important property of such a spectral basis is that its errors go to zero exponentially with the number of degrees of freedom.

We also use a method based on integration of the mean ST, evaluated in terms of the imaginary-frequency Green's function via the fluctuation-dissipation theorem [13]. The Green's function can be evaluated by a variety of techniques [13], but here we use a simple finite-difference frequency-domain method (FDFD) [17] that has the advantage of being very general and simple to implement at the expense of efficiency—it is much less efficient for this specific geometry than the PI method. The results from both methods are shown in Fig. 1, with the PI method indicated by solid and dashed lines for two and one sidewalls, respectively, and the ST method indicated by data points. Both results agree to within the numerical accuracy, as expected, although we have fewer data points (and larger error bars) from the ST method because it is less efficient for this geometry. We focus on the interpretation of the results rather than on the computational techniques.

To begin with, we compute the force between the two cylinders (with $a/R=2$) as a function of the sidewall separation h/a, for fixed a. The results, for both one sidewall (solid lines) and two sidewalls (dashed lines) are shown in Fig. 1 for the total force, and also the forces for the individual polarizations TE and TM. The forces are all normalized to the PFA result between two cylinders [18], which is independent of h and does not affect the shape of the curves in Fig. 1. Two interesting observations can be made from this figure. First, the total force (for both one and two sidewalls) is a nonmonotonic function of h/R: at first decreasing and then increasing towards the asymptotic limit between two isolated cylinders. The extremum for the one-sidewall case occurs at $h/R\approx 0.27$, and for the two-sidewall case is at $h/R\approx 0.46$ (similar to the $h/R\approx 0.5$ for squares between two sidewalls [9]). Second, the total force for the two-sidewall case in the $h=0$ limit is larger than for $h\to\infty$. As might be expected, the h-dependence for one sidewall is weaker than for two sidewalls, and the effects of the two sidewalls are not additive: not only is the difference from $h\to\infty$ force not doubled for two sidewalls compared to one, but the two curves actually intersect at one point.

Since nonmonotonic sidewall effects appear to occur for a variety of shapes (both for square [9] and circular cross sections), it is natural to seek a simple generic argument to explain this phenomenon. As we see in Fig. 1, and also in our earlier work [9], the nonmonotonicity arises from a competition between the TE and TM force contributions: the TE force is quickly decreasing with h while the TM force is slowly increasing. Therefore, an underlying question is why the TE force increases as the sidewall comes closer, while the TM force decreases.

An intuitive perspective of the effects of the metallic sidewall(s) on the TE and/or TM forces is obtained from the "method of images," whereby the boundary conditions at the plate(s) are enforced by appropriate image sources. For the Dirichlet boundary conditions (TM polarization) the image charges have *opposite* signs, and the potential due to a charge (more precisely, the Green's function at any imaginary frequency, which determines the Casimir force) is obtained by subtracting the contribution from the opposing image. Any configuration of fluctuating TM charges on one cylinder is thus screened by images, more so as h is decreased, *reducing* the force on the fluctuating charges of the second cylinder [33]. Since the reduction in force is present for every configuration, it is there also for the average over all configurations, accounting for the variations of the TM curves in Fig. 1. By contrast, the Neumann boundary conditions (TE polarization) require image sources (current loops) of the *same* sign. The total force between fluctuating currents on the cylinders is now larger and increases as the plate separation h is reduced. (An analogous additive effect occurs for the classical force between current loops near a conducting plane.)

Note, however, that while for each fluctuating source configuration, the effect of images is additive, this is no longer the case for the average over all configurations. More precisely, the effect of an image source on the Green's function

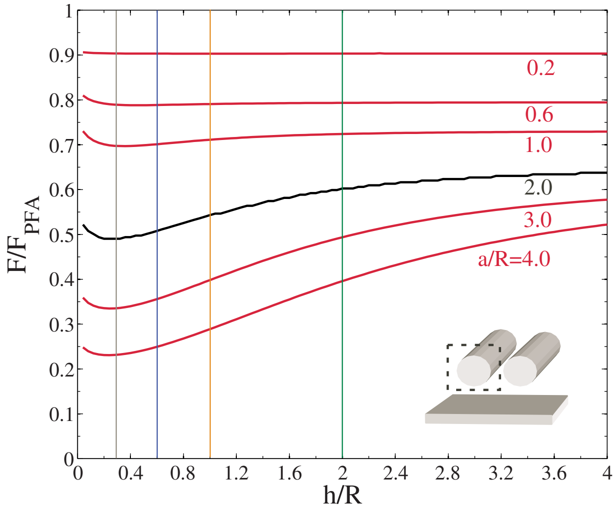

FIG. 2. (Color online) Casimir force per unit length between two cylinders of fixed radius R vs the ratio of sidewall separation to cylinder radius h/R (for one plate), normalized by the total PFA force per unit length between two isolated cylinders. The force is plotted for different cylinder separations of a/R=0.2, 0.6, 1.0, 2.0, 3.0, and 4.0.

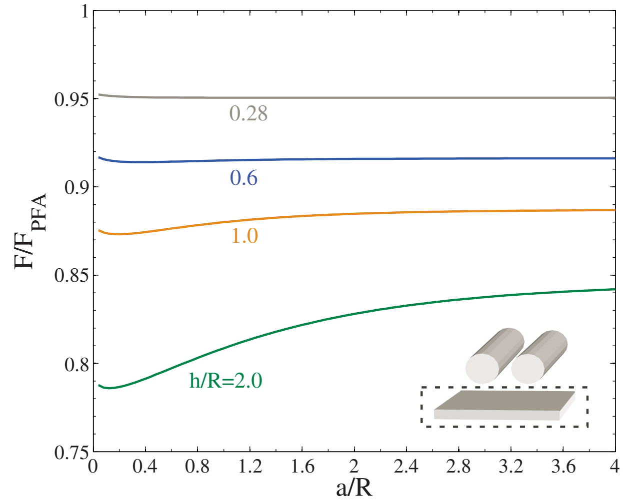

FIG. 3. (Color online) Casimir force per unit length between a plate and two cylinders of fixed radius R vs the ratio of cylinder separation to cylinder radius a/R, normalized by the total PFA force per unit length between a cylinder and a plate $F_{\text{PFA}} = \frac{5}{2}(\hbar c \pi^3/960)\sqrt{R/2a^7}$ [19]. The force is plotted for different plate separations of h/R=0.28, 0.6, 1.0, and 2.0. Note that the normalization is different from the cylinder-cylinder PFA in the previous figures.

is not additive because of feedback effects: the image currents change the surface current distribution, which changes the image, and so forth. For example, the net effect of the plate on the Casimir TE force *is not* to double the force as $h\to 0$. The increase is in fact larger than two due to the correlated fluctuations.

While the method of images explains the competition between TE and TM modes that underlies the nonmonotonic effects, further considerations are required to ensure that their sum is nonmonotonic. For example, if the TE and TM variations with h were equal and opposite, they would cancel with no net dependence on h. That this is not the case can be checked by examining the limit $a \gg h \gg R$. In this limit the forces are dominated by the lowest spectral (Fourier) mode, s wave for TM and p wave for TE [10]. The former is stronger and leads to an asymptotic form (for one plate):

$$\frac{F}{L} = -\frac{4\hbar c}{\pi}\frac{h^4}{a^7 \ln^2(R/h)}, \tag{1}$$

confirming the reduced net force as the cylinders approach the plate. While the logarithmic dependence on R could have been anticipated [10], the h^4 scaling is a remarkable consequence of the multibody effect. Each cylinder and its mirror image can be considered as a dipole of size $\sim h$. The interaction of the two dipoles should scale as the interaction between two cylinders of size $\sim h$ with Neumann boundary conditions. For $a \gg h$ the force for the latter problem scales as $\sim h^4/a^7$, explaining the above result [10], up to the logarithm. To analytically establish the nonmonotonic character, we also need to show that the TE force is dominant in the opposite limit of $h \ll R$. So far, we only have our numerical results of Fig. 1 in favor of this.

In Fig. 2, we show the total force vs h/R for a variety of different values of the cylinder separation a in the presence of a single sidewall. The value $a/R=2$ corresponds to our previous results in Fig. 1. Note that if a is too large or too small, the degree of nonmonotonicity (defined as the difference between the minimum force and the $h=0$ force) decreases. [For small a, the force is accurately described by PFA, while for large a the TM mode dominates as indicated in Eq. (1).] The separation $a/R=2$ from Fig. 1 seems to achieve the largest value of nonmonotonicity.

When the force between the cylinders is not monotonic in h, it also follows that the force between the cylinders and the sidewalls is not monotonic in a. A nonmonotonic force F_x between the cylinders means that there is a value of h where $dF_x/dh=0$. Since the force is the derivative of the energy, $F_x=-\partial\mathcal{E}/\partial a$, at this point $\partial^2\mathcal{E}/\partial a\,\partial h=0$. These two derivatives, of course, can be interchanged to obtain $\partial(\partial\mathcal{E}/\partial h)/\partial a=0$. But this means that $dF_y/da=0$ at the same point, where $F_y=-\partial\mathcal{E}/\partial h$ is the force between the cylinders and the sidewall. This cylinders-sidewall force is plotted in Fig. 3 as a function of a/R for various values of h/R. (It is not surprising that the effect of a small cylinder on the force between two bodies is smaller than the effect of an infinite plate. In future work we also show that the cylinder-cylinder force is generally less than the cylinder-plate force for the same cylinder diameter and surface separation [18].)

The advantage of the cylinder-plate force compared to the cylinder-cylinder force is that it seems operationally closer to the sphere-plate geometries that have been realized experimentally. In order to measure the cylinder-cylinder force, one would need to suspend two long cylinders in vacuum nearly parallel to one another. To measure the cylinder-plate force, the cylinders need not be separated by vacuum—we expect that a similar phenomenon will arise if the cylinders are separated by a thin dielectric spacer layer. Unfortunately, the nonmonotonic effect in Fig. 3 is rather small (roughly 0.2%), but it may be possible to increase this by further optimization of the geometry. In future calculations, we also hope to determine whether the same phenomenon occurs for two spheres next to a metal plate.

Our aim in this paper has been to establish the existence of nonmonotonic and non-two-body Casimir forces as a matter of principle. If, however, one were to attempt to observe these effects experimentally, one would need to take into account thermal fluctuations, surface roughness, and finite thermal conductivity. This has been undertaken for other geometries [10,19–27]; for a review of the controversy on finite conductivity calculations, see [28]. For the typical length scales studied experimentally the roughness corrections are assumed to be small, while thermal fluctuations ought to be unimportant in the submicron range. Of course, issues of parallel or skewed alignment in experiments are present in a similar manner for other geometries as has been discussed thoroughly by other authors [19,20].

In previous research, unusual Casimir force phenomena were sought by considering parallel plates with exotic materials: for example, repulsive forces were predicted using magnetic conductors [29], combinations of different dielectrics [30], fluids between the plates [31], and even negative-index media with gain [32]. A different approach is to use ordinary materials with more complicated geometries: as illustrated in this and previous [9] work, surprising nonmonotonic (attractive) effects can arise by considering as few as three objects.

This work was supported in part by NSF Grant No. DMR-04-26677 (S.J.R. and M.K.), by the U.S. Department of Energy (DOE) under cooperative research agreement Contract No. DF-FC02-94ER40818 (R.L.J.), by DOE Grant No. DE-FG02-97ER25308 (A.W.R.), and by DFG Grant No. EM70/3 (T.E.).

[1] H. B. G. Casimir, Proc. K. Ned. Akad. Wet. **51**, 793 (1948).
[2] E. M. Lifshitz and L. P. Pitaevskii, *Statistical Physics: Part 2* (Pergamon, Oxford, 1980).
[3] R. Onofrio, New J. Phys. **8**, 237 (2006).
[4] F. Capasso, J. N. Munday, D. Iannuzzi, and H. B. Chan, IEEE J. Sel. Top. Quantum Electron. **13**, 400 (2007).
[5] M. Bordag, Phys. Rev. D **73**, 125018 (2006).
[6] V. A. Parsegian, *Van der Waals Forces: A Handbook for Biologists, Chemists, Engineers, and Physicists* (Cambridge University Press, New York, 2006).
[7] H. B. G. Casimir and D. Polder, Phys. Rev. **73**, 360 (1948).
[8] R. Sedmik, I. Vasiljevich, and M. Tajmar, J. Comput.-Aided Mater. Des. **14**, 119 (2007).
[9] A. Rodriguez, M. Ibanescu, D. Iannuzzi, F. Capasso, J. D. Joannopoulos, and S. G. Johnson, Phys. Rev. Lett. **99**, 080401 (2007).
[10] T. Emig, R. L. Jaffe, M. Kardar, and A. Scardicchio, Phys. Rev. Lett. **96**, 080403 (2006).
[11] S. Zaheer, A. W. Rodriguez, S. G. Johnson, and R. L. Jaffe, Phys. Rev. A **76**, 063816 (2007).
[12] R. E. Collin, *Field Theory of Guided Waves*, 2nd ed. (IEEE, New York, 1991).
[13] A. Rodriguez, M. Ibanescu, D. Iannuzzi, J. D. Joannopoulos, and S. G. Johnson, Phys. Rev. A **76**, 032106 (2007).
[14] R. Büscher and T. Emig, Phys. Rev. Lett. **94**, 133901 (2005).
[15] T. Emig, A. Hanke, R. Golestanian, and M. Kardar, Phys. Rev. A **67**, 022114 (2003).
[16] D. A. R. Dalvit, F. C. Lombardo, F. D. Mazzitelli, and R. Onofrio, Phys. Rev. A **74**, 020101(R) (2006).
[17] A. Christ and H. L. Hartnagel, IEEE Trans. Microwave Theory Tech. **35**, 688 (1987).
[18] S. J. Rahi, T. Emig, R. L. Jaffe, and M. Kardar (unpublished).
[19] D. A. R. Dalvit, F. C. Lombardo, F. D. Mazzitelli, and R. Onofrio, Europhys. Lett. **67**, 517 (2004).
[20] M. Brown-Hayes, D. A. R. Dalvit, F. D. Mazzitelli, W. J. Kim, and R. Onofrio, Phys. Rev. A **72**, 052102 (2005).
[21] I. Brevik, J. B. Aarseth, J. S. Høye, and K. A. Milton, Phys. Rev. E **71**, 056101 (2005).
[22] M. Boström and B. E. Sernelius, Phys. Rev. Lett. **84**, 4757 (2000).
[23] F. Chen, G. L. Klimchitskaya, U. Mohideen, and V. M. Mostepanenko, Phys. Rev. Lett. **90**, 160404 (2003).
[24] B. Geyer, G. L. Klimchitskaya, and V. M. Mostepanenko, Phys. Rev. A **67**, 062102 (2003).
[25] B. Geyer, G. L. Klimchitskaya, and V. M. Mostepanenko, Phys. Rev. A **65**, 062109 (2002).
[26] G. L. Klimchitskaya, U. Mohideen, and V. M. Mostepanenko, Phys. Rev. A **61**, 062107 (2000).
[27] F. Chen, G. L. Klimchitskaya, V. M. Mostepanenko, and U. Mohideen, Phys. Rev. B **76**, 035338 (2007).
[28] V. M. Mostepanenko, V. B. Bezerra, R. S. Decca, B. Geyer, E. Fischbach, G. L. Klimchitskaya, D. E. Krause, D. López, and C. Romero, J. Phys. A **39**, 6589 (2006).
[29] O. Kenneth, I. Klich, A. Mann, and M. Revzen, Phys. Rev. Lett. **89**, 033001 (2002).
[30] Y. Imry, Phys. Rev. Lett. **95**, 080404 (2005).
[31] J. N. Munday and F. Capasso, Phys. Rev. A **75**, 060102(R) (2007).
[32] U. Leonhardt and T. G. Philbin, New J. Phys. **9**, 254 (2007).
[33] A key fact is that the Green's functions in Casimir forces are naturally evaluated at imaginary frequencies [13], which means that they are decaying and not oscillating. If they were oscillating, one could not as easily infer whether opposite-sign image currents add or subtract.